

Supporting information

Rapid and selective adsorption of gold ions with hydroxyl functionalized UiO-66-type metal-organic framework

Wenhui Yao, Yongkui Chen* and Xiaowei Guo

School of Chemistry and Chemical Engineering, Xinxiang University, Xinxiang, Henan 453003, P. R. China

Corresponding author. Email: chenyongkui198002@xxu.edu.cn

Fig. S1 Thermogravimetric analysis trace of UiO-66-(OH)_2 .

Fig. S2 PXRD patterns of UiO-66-OH .

Fig. S3 FTIR spectroscopy of UiO-66-OH .

Fig. S4 N_2 adsorption isotherm of UiO-66-OH at 77 K (insert: pore size distribution).

Fig. S5 Thermogravimetric analysis trace of UiO-66-(OH) .

Fig. S6 Linear fitting curve using pseudo-first-order model on UiO-66-(OH)_2 (0-240 min).

Fig. S7 Kinetic study of Au (III) adsorption on UiO-66-OH .

Fig. S8 Linear fitting curve using pseudo-second-order model on UiO-66-OH (0-240 min).

Fig. S9 Linear fitting curve using pseudo-first-order model on UiO-66-OH (0-240 min).

Fig. S10 Freundlich isotherm model fitting Au (III) on UiO-66-(OH)_2 .

Fig. S11. Adsorption isotherm of Au (III) on UiO-66-OH ($\text{pH} = 6$, $t = 4$ h, $T = 25^\circ\text{C}$).

Fig. S12 Langmuir isotherm model fitting of Au (III) on UiO-66-OH .

Fig. S13 Freundlich isotherm model fitting of Au (III) on UiO-66-OH .

Fig. S14 PXRD patterns of UiO-66-(OH)_2 after 5 adsorption-desorption cycles.

Fig. S15. SEM image of UiO-66-(OH)_2 after gold adsorption.

Fig. S16. SEM energy-dispersive X-ray spectroscopy (EDS) elemental mapping images of UiO-66-(OH)_2 after gold adsorption.

Fig. S17 FTIR spectroscopy comparison of UiO-66-(OH)_2 before and after adsorption.

Table S1 Kinetics model parameters of gold adsorption on MOFs at 25°C and $\text{pH} = 6.0$.

Table S2 Parameters of the fitted Au (III) adsorption isotherms using Langmuir and Freundlich models.

Table S3 Comparison of the equilibrium time and adsorption capacity of various adsorbents for the extraction of gold ions.

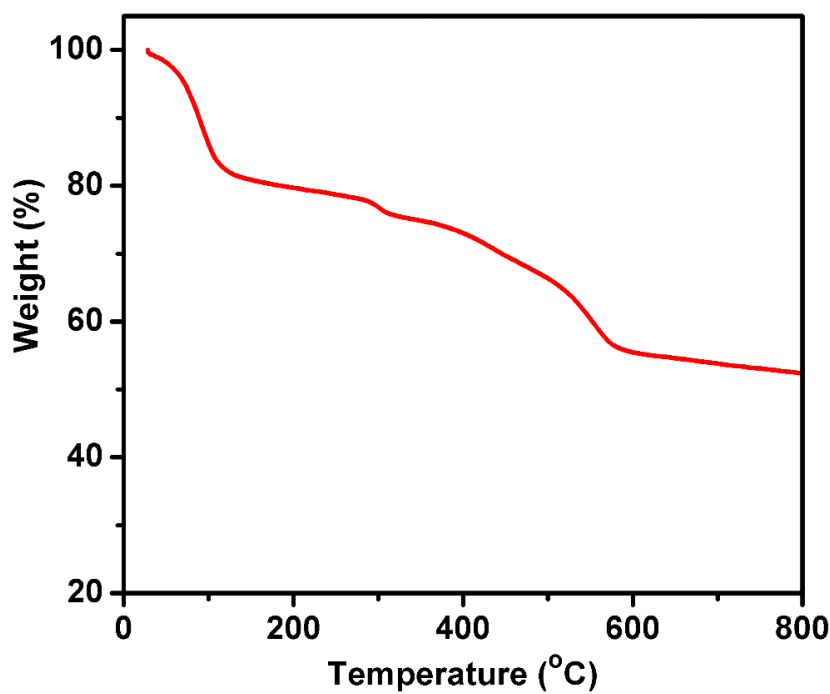


Fig. S1 Thermogravimetric analysis trace of UiO-66-(OH)₂.

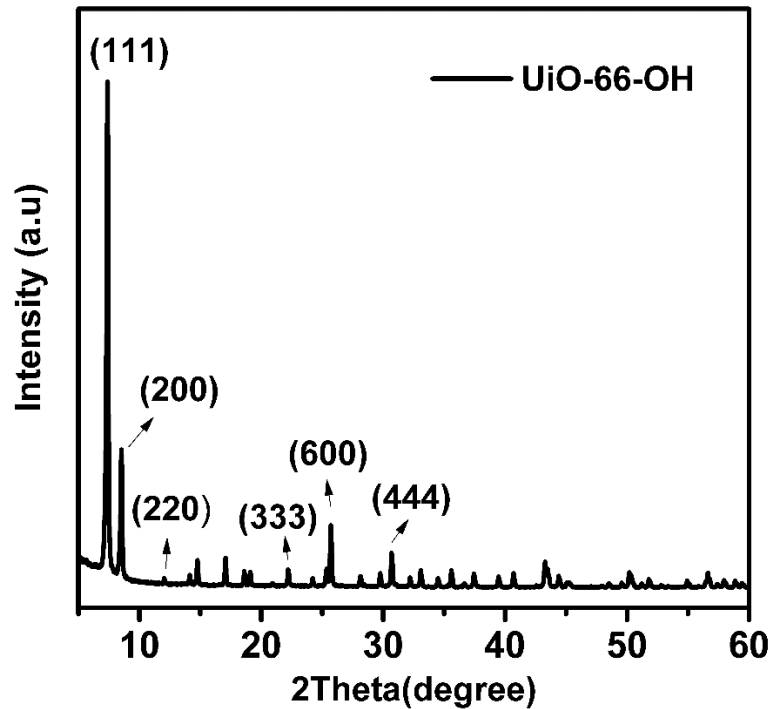


Fig. S2 PXRD patterns of UiO-66-OH, where two major diffraction peaks appeared at approximate 7.4 and 8.5° , corresponding to the crystal planes (111) and (200), and the moderate peaks positioned at about 12.0° (220), 22.2° (333), 25.6° (600) and

30.6° (444).

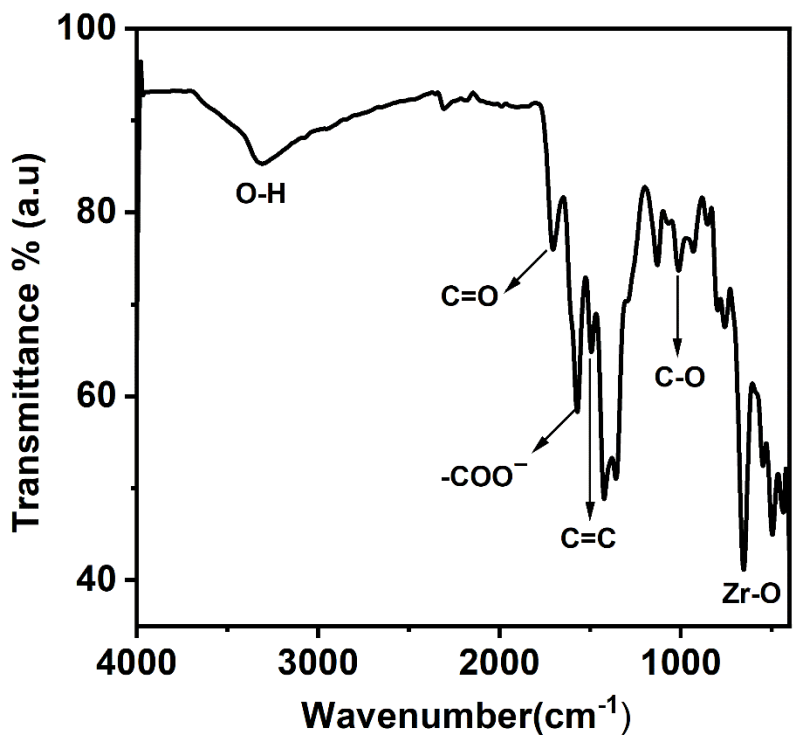


Fig. S3 FTIR spectroscopy of UiO-66-OH.

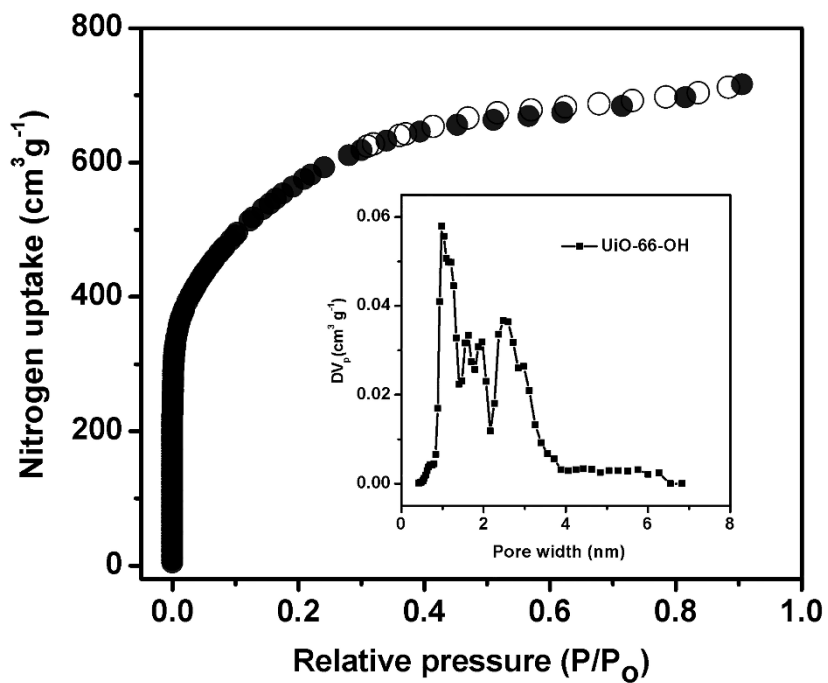


Fig. S4 N₂ adsorption isotherm of UiO-66-OH at 77 K (insert: pore size distribution).

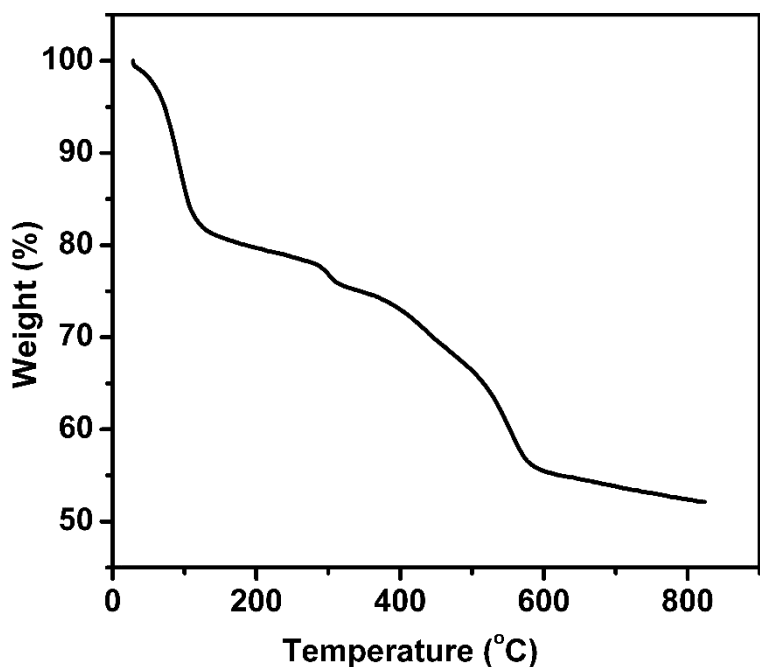


Fig. S5 Thermogravimetric analysis trace of UiO-66-(OH), where the minor mass loss below 100°C due to the desorption of physically adsorbed water molecules and/or residual solvent from the MOF pores.

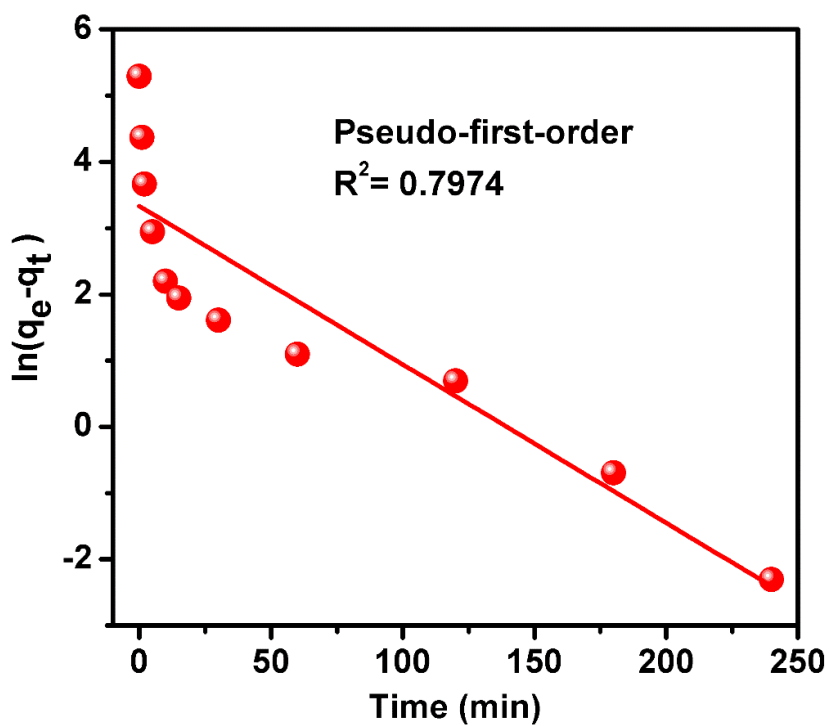


Fig. S6 Linear fitting curve using pseudo-first-order model on UiO-66-(OH)_2 (0-240 min).

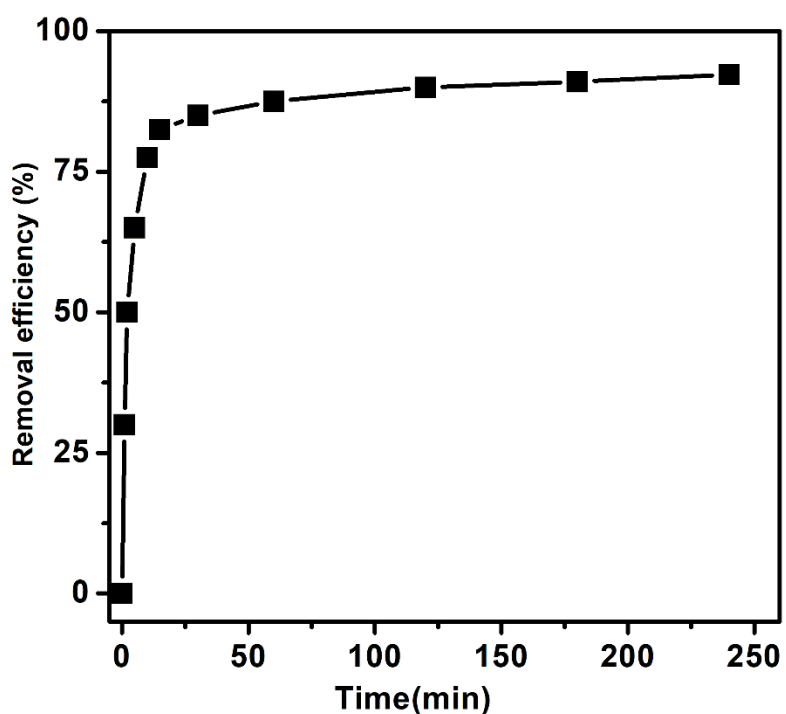


Fig. S7 Kinetic study of Au (III) adsorption on UiO-66-OH.

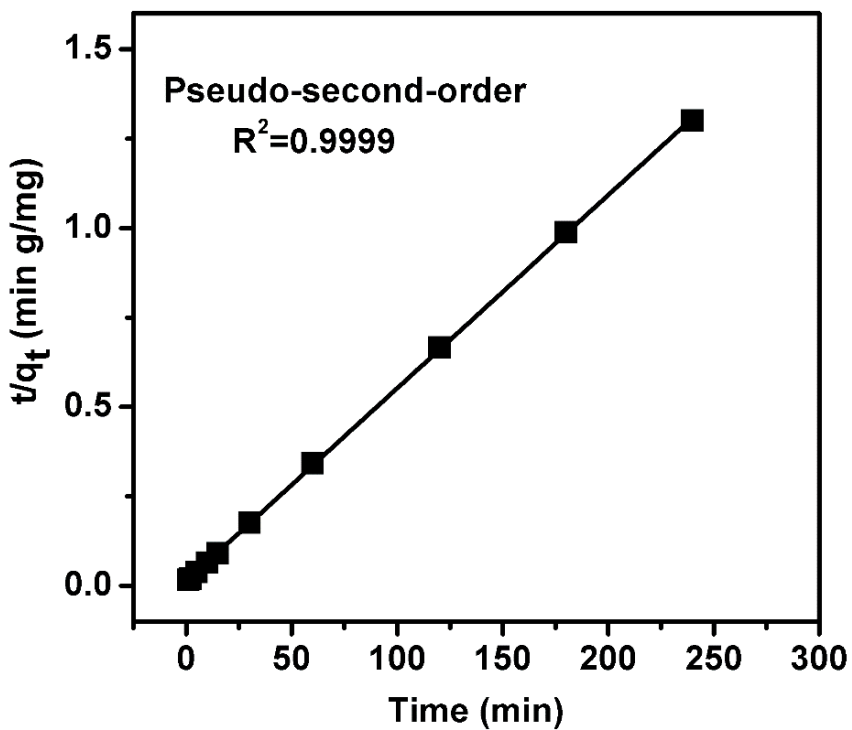


Fig. S8 Linear fitting curve using pseudo-second-order model on UiO-66-OH (0-240

min).

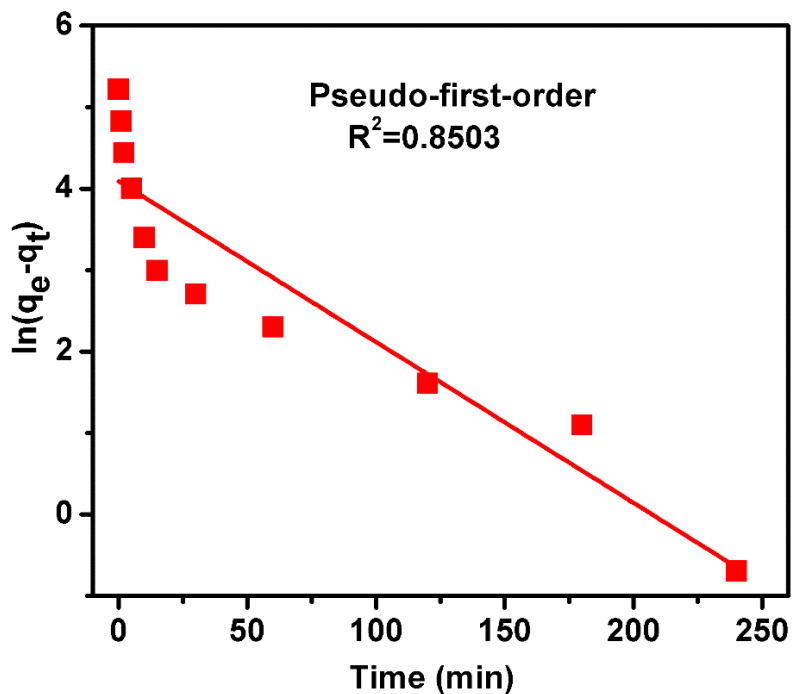


Fig. S9 Linear fitting curve using pseudo-first-order model on UiO-66-OH (0-240 min).

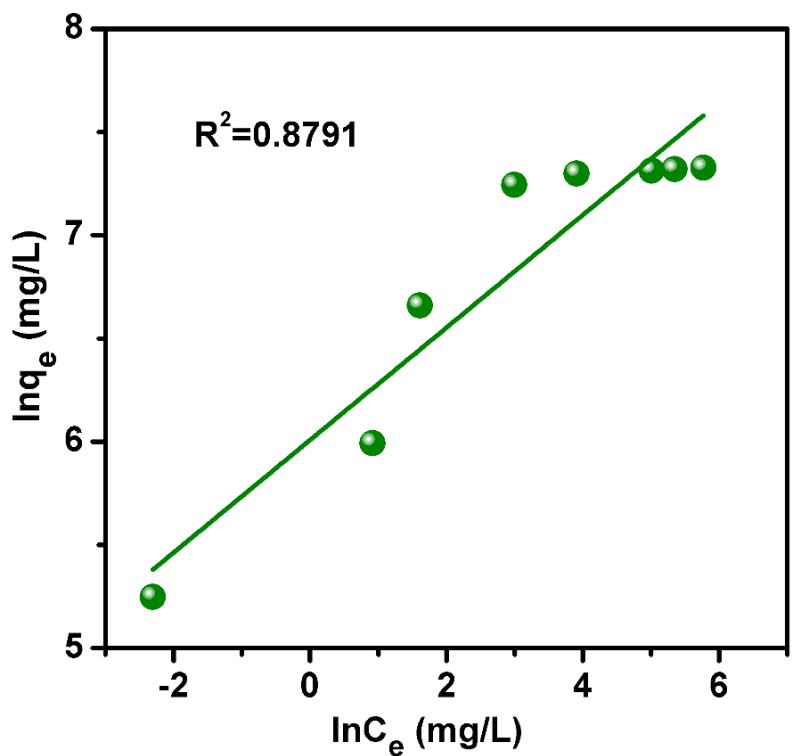


Fig. S10 Freundlich isotherm model fitting Au (III) on UiO-66-(OH)₂.

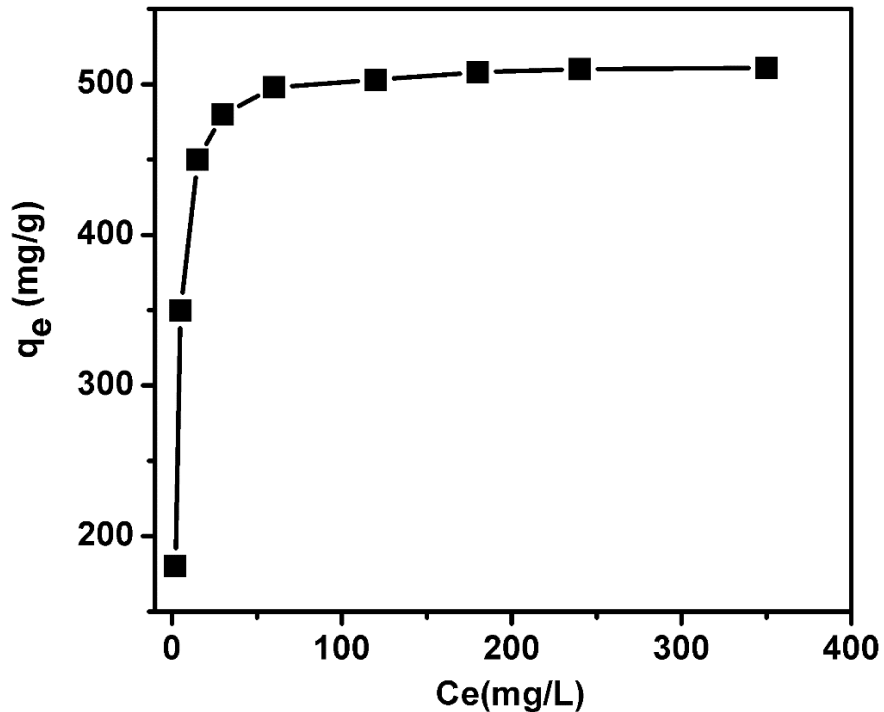


Fig. S11 Adsorption isotherm of Au (III) on UiO-66-OH (pH = 6, t = 4 h, T = 25 °C).

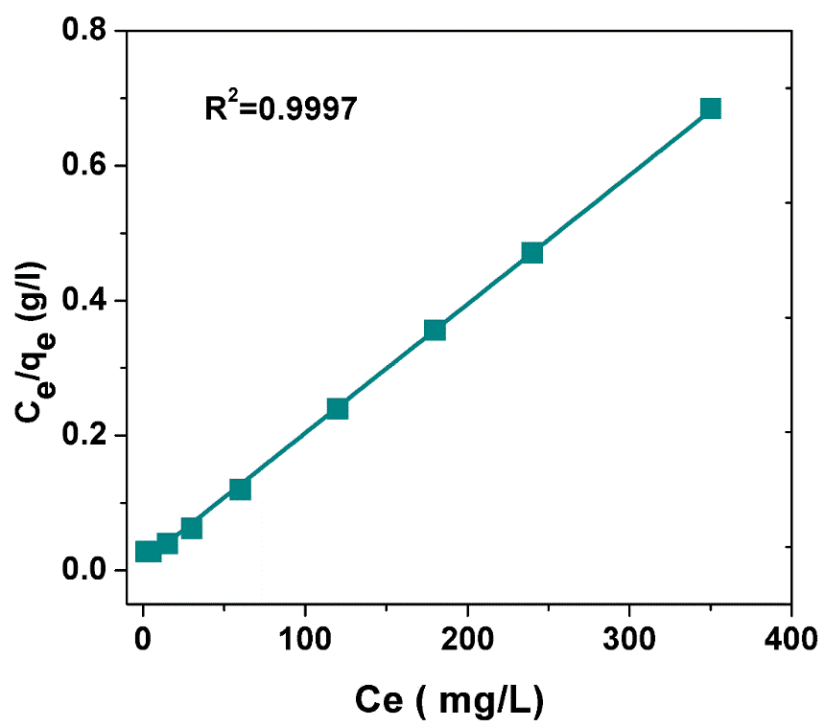


Fig. S12 Langmuir isotherm model fitting of Au (III) on UiO-66-OH

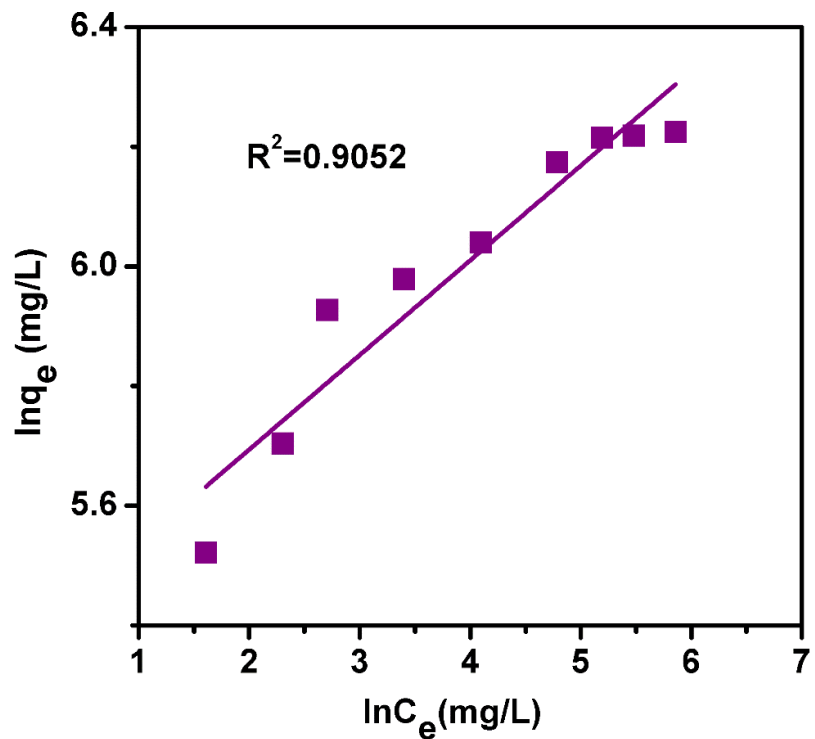


Fig. S13 Freundlich isotherm model fitting of Au (III) on UiO-66-OH

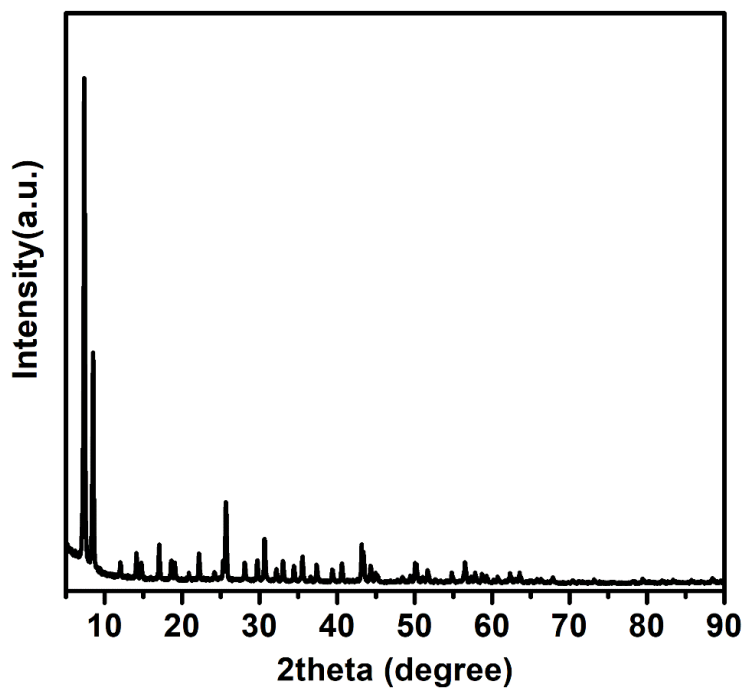


Fig. S14 PXRD patterns of UiO-66-(OH)₂ after 5 adsorption-desorption cycles.

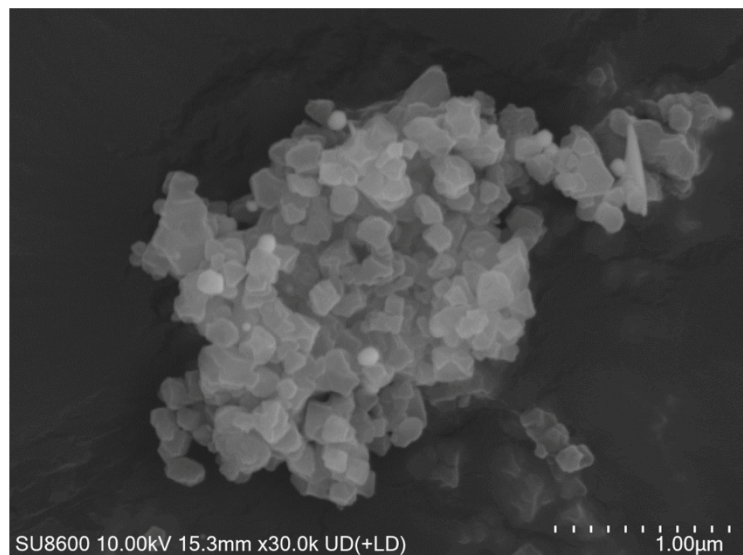


Fig. S15. SEM image of UiO-66-(OH)₂ after gold adsorption.

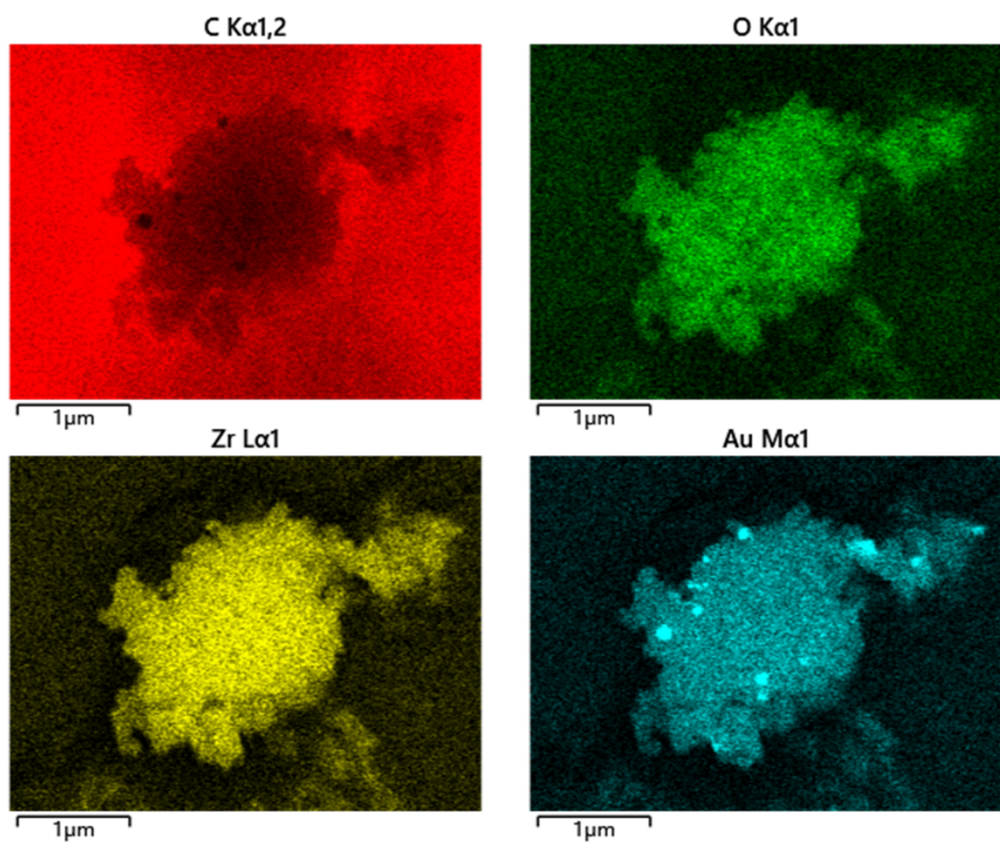


Fig. S16. SEM energy-dispersive X-ray spectroscopy (EDS) elemental mapping

images of UiO-66-(OH)₂ after gold adsorption.

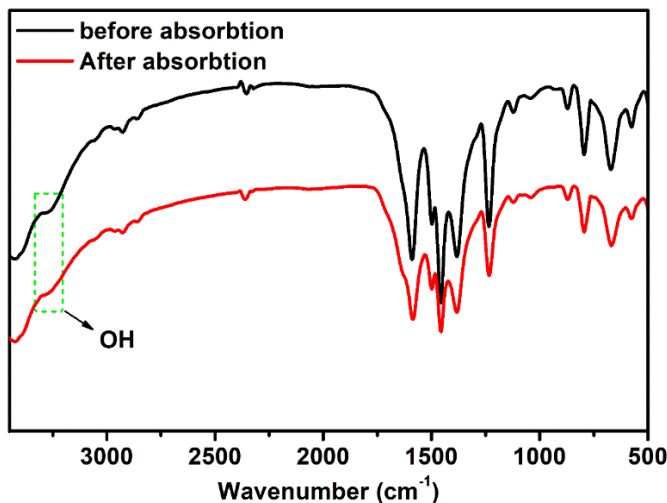


Fig. S17 FTIR spectroscopy comparison of UiO-66-(OH)₂ before and after adsorption.

Table S1 Kinetics model parameters of gold adsorption on MOFs at 25 °C and pH = 6.0.

MOF	Pseudo-first-order model			Pseudo-second-order model		
	Q _e (mg g ⁻¹)	K ₁ (min ⁻¹)	R ²	q _e (mg g ⁻¹)	K ₂ (gmin ⁻¹ mg ⁻¹)	R ²
UiO-66-OH	49.40	0.01859	0.8503	184.5	0.0022	0.9999
UiO-66-(OH) ₂	27.93	0.02393	0.7974	199.2	0.0073	0.9999

Table S2 Parameters of the fitted Au (III) adsorption isotherms using Langmuir and Freundlich models.

Isotherm model	MOF	Isotherm model		
		q _m (mg/g)	K _L (L/mg)	R ²
Langmuir model	UiO-66-OH	523.6	0.1494	0.9997
	UiO-66-(OH) ₂	1571.5	0.1550	0.9999
		K _F	n	R ²

Freundlich model	UiO-66-OH	216.4	6.32	0.9052
	UiO-66-(OH) ₂	406.3	3.67	0.8791

Table S3 Comparison of the equilibrium time and adsorption capacity of various adsorbents for the extraction of gold ions

Absorbents	Equilibrium time (min)	q _m (mg/g)	reference
BMTA-TFPM-COF	30	570.18	1
TzDa-COF	30	1866	2
JNM-100-AO	10	954	3
2,5-TP	960	1253.5	4
A-PGMA	180	441	5
UiO-66-TA	240	372	6
TP-AFC	840	881	7
UiO-66-TU	90	326	8
UiO-66-BTU	240	680	9
Methionine-MOFs	60	598	10
Aliquat-336 impregnated alginate capsule	1440	192	11
Thiosemicarbazide functionalized corn bract	1440	1472	12
Fe ₃ O ₄ @DMSA	480	296	13
UiO-66-NH ₂	120	604	14
UiO-66-OH	10	520	This work
UiO-66-(OH) ₂	10	1570	This work

- 1 M. Liu, H. Y. Kong, S. Bi, X. Ding, G. Z. Chen, J. He, Q. Xu, B.- H. Han and G. Zeng, *Adv. Funct. Mater.*, 2023, **33**, 2302637.
- 2 S. Zhong, Y. Wang, T. Bo, J. Lan, Z. Zhang, L. Sheng, J. Peng, L. Zhao, L. Yuan, M. Zhai and W. Shi, *Chem. Eng. J.*, 2023, **455**, 140523.
- 3 J. Luo, X. Luo, M. Xie, H.-Z. Li, H. Duan, H.-G. Zhou, R.-J. Wei, G.-H. Ning and D. Li, *Nat. Commun.*, 2022, **13**, 7771.

- 4 C. Hu, W. Xu, H. Li, S. Zhou, X. Mo , P. Zhang and K.Tang, *Ind. Eng. Chem. Res.* 2019, **58**, 17972-17979.
- 5 C, Xiong, S. Wang, L. Zhang, L.Ying , Z. Yang and J.Peng, *Polymers*, 2018, **10**, 159.
- 6 C. Wang, G. Lin, J. Zhao, S. Wang, L. Zhang, Y. Xi, X. Li and Y. Ying, *Chem. Eng. J.*, 2020, **380**, 122511.
- 7 C. Wang, J. Zhao, S. Wang, L. Zhang and B. Zhang. *Polymers*, 2019, **11**, 652.
- 8 C. Wu, X. Zhu, Z. Wang, J. Yang, Y. Li and J. Gu, *Ind. Eng. Chem. Res.*, 2017, **56**, 13975–13982.
- 9 J. Guo, X. Fan, J. Wang, S. Yu, M. Laipan, X. Ren, C. Zhang, L. Zhang and Y. Li, *Chem. Eng. J.*, 2021, **425**, 130588.
- 10 M. Mon, J. Ferrando-Soria, T. Grancha, F. R. Fortea-Pérez, J. Gascon, A. Leyva-Pérez, D. Armentano and E. Pardo, *J. Am. Chem. Soc.*, 2016, **138**, 7864–7867.
- 11 W. Wei, D. H. K. Reddy, J. K. Bediako and Y.-S. Yun, *Chem. Eng. J.*, 2016, **289**, 413–422.
- 12 G. Lin, S. Wang, L. Zhang, T. Hu, J. Peng, S. Cheng and L. Fu, *J. Mol. Liq.*, 2018, **258**, 235–243.
- 13 O. F. Odio, L. Lartundo-Rojas, P. Santiago-Jacinto, R. Martínez and E. Reguera, *J. Phys. Chem. C*, 2014, **118**, 2776–2791.
- 14 J. Cao, Z. Xu, Y. Chen, S. Li, Y. Jiang, L. Bai, H. Yu, H. Li and Z. Bian, *Angew. Chem. Int. Ed.*, 2023, **62**, e202302202.